Rear slant angle optimization for road vehicle aerodynamics (Ahmed Body)

- Drag reduction using RANS turbulence model

Abhishek Dhiman (abhdh352), Tarun Teja (tarna588), Yeshwanth Yammada (sanna002)

INTRODUCTION

The evolution of ground vehicles aerodynamics has secured significant attention over the years. Increment in aerodynamic efficiency directly influences fuel consumption and the economic expectation from a modern car. The most investigated generic bluff body (Ahmed Body) is studied using Computational Fluid Dynamics (CFD) to analyze the salient flow features contributing to aerodynamic drag. The primary aim is to perform validation of lift and drag coefficient on each surface of Ahmed body against the Large Eddy Simulation (LES) data for slant angle (φ) = 35◦. Secondary focal point is the optimization of the slant angle (at car C-pillar) for minimum/maximum drag followed by the influence of the aspect ratio (width / height) of Ahmed body. The flow behavior at 35◦ slant angle along with critical angles (12.5◦ & 30◦) [1] [2] have been heavily investigated in the existing literature and hence held fundamental importance.

METHOD

Scaled-down ($\frac{1}{4}$) model of the Ahmed body slant angle (ϕ) = $35°$ is taken as the baseline for the modeling approach. Ahmed body is encased in a domain of dimension [length = 8.45L, breadth = 1.15L, height = 2.33L], where L is the longitudinal length of Ahmed body. Two inner refinement regions are also created for better mesh growth away from Ahmed body. Analysis of various slant angles in the range [$5°$- $53°$] is performed to find the best and worst slant angles leading to minimum and maximum drag coefficients respectively. Also, the aspect ratio (width/height) of Ahmed body is examined to estimate its impact on the drag coefficient (C_d) of the body. Complied with the requirement of a maximum 512K (512,000) nodes in the mesh, symmetry condition is employed to generate a good-quality mesh (M3) with 455.5K nodes. The mesh verification details are presented in *Table.1***,** where M3 showed 4.41% GCI for C_d and 69.23% for C_l. The C_d is comparatively important for the study and C_l showed oscillatory behavior, hence M3 is selected. Two domains around the Ahmed body (inner and outer) are used to achieve significantly higher mesh density near the body of interest to better resolve the gradients of flow variables. In the inner region, the patch-conforming method is utilized with the implementation of tetrahedron elements. Inflation is applied on all the Ahmed body surfaces (20 layers) and ground (10 layers) to achieve the $y^+ < 1$ and $y^+ < 5$ respectively in order to capture the near wall flow physics and boundary layer effects. Body sizing mesh is used to achieve multiple layers of tetrahedrons elements between the car body and ground inflation layers leading to a better element growth rate and information transfer between ground and the Ahmed body.

Table. 1: Mesh Verification

Mesh	Nodes	h	r	C_d	GCI C_d%	C_l	GCI C_l%
M1	53037	11.5		0.493		-0.005	
M2	155150	8.4	1.38	0.381	13.6	-0.035	273.5
M3	455438	5.73	1.47	0.353	4.41	-0.092	69.23

Steady state Reynolds Average Navier-Stokes (RANS) simulation with Shear Stress Transport (SST) turbulence model also called k-ω SST is utilized to capture salient features of boundary layer on the surface aided with y^+ values mentioned above. In Ansys CFX R22, High resolution with 1st order turbulence numeric is employed which internally use 2nd order UPWIND discretization scheme controlled by a blend factor ($0 < \beta < 1$) with value close to 1 to avoid new extrema implying maintained boundedness and reduce the convergence issues. For continuity and momentum also, High Resolution advection scheme is used. The $R_{e_{\sqrt{A}}} = 30000$ is used, where A is the frontal area of the Ahmed body and a convergence criterion of 10^{-5} is achieved for all the simulation with a time scale factor of 0.25.

RESULTS & DISCUSSION

Model verification showed discretization error for C_d is in acceptable range (< 5%) but the C_l it is

significantly high due to periodic oscillation resulting in convergence issue for C_l. Hence, reducing the method credibility for C_l prediction. Model validation is performed against the available Large Eddy Simulations (LES) data, ***Fig*** *[1, 2]*. Comparison between SST model and LES showed good agreement for all surfaces for $C_{l_{Total}}$ and $C_{d_{Total}}$ ***Fig*** *[1a, 1b]*. The exception seen is at front and back surface with high under-prediction of $C_{d_{Total}}$ and bottom surface for $C_{l_{Total}}$. The C_l had trivial impact from side and back surfaces.

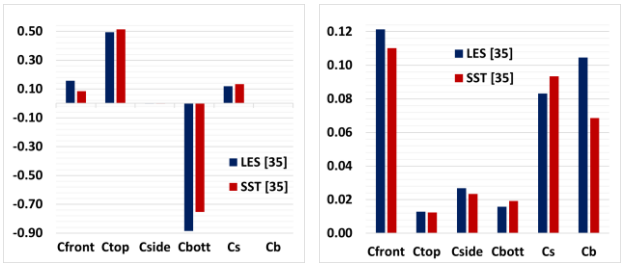

1a. Surface $C_{l_{Total}}$ **1b.** Surface $C_{d_{Total}}$

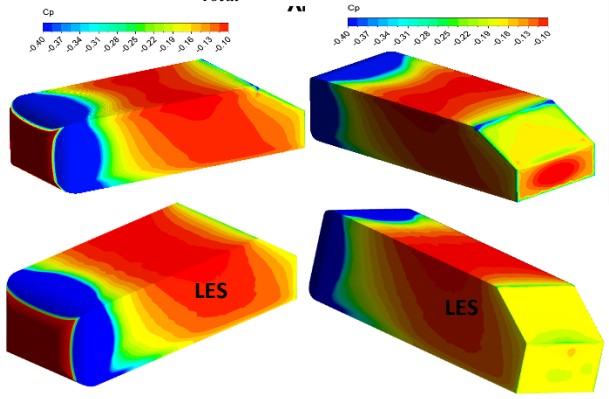

1c. Surface pressure coefficient contour comparison

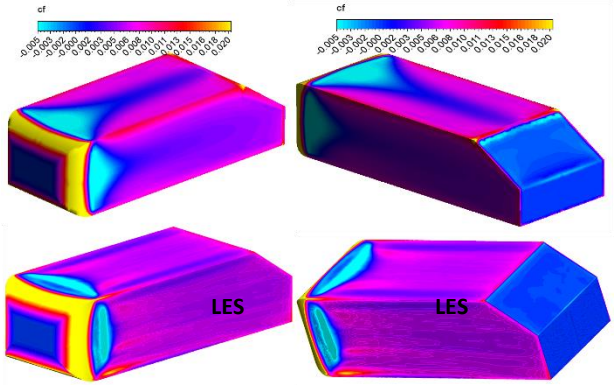

1d. Surface skin friction coefficient contour comparison

Fig. **1:** C_l & C_d, C_p and C_f comparison at ϕ = 35° between SST and LES data

The front, top and slant generate vertical-up force, and only bottom surface contributing to the generation of the vertical-down force, ***Fig****. 1a*. The validation of C_p agreed well with LES data *Fig. 1c*, with front and slant faces underestimated. For C_f in *Fig. 1d*, the agreement is good on all surfaces except the front and marginal underestimation on top face. The poor estimation on front and slant faces can be related to the discretization error and complex flow structures on these faces. The overall estimation of C_d on Ahmed body is in good agreement w.r.t LES, but noteworthy C_l deviations infer to low credibility of the model *Fig. 2*.

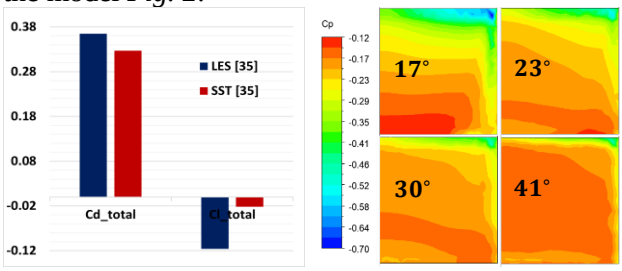

Fig.2 : $C_{l_{Total}}$ and $C_{d_{Total}}$ comparison between LES & SST [left], and Pressure coefficient (C_p) over slant surface [SST]

Subsequently, slant angle range [5°<= ϕ <= 53°] is analyzed for total drag $C_{d_{Total}}$ ***Fig****. 3a*, along with component break down into $C_{d_{pressure}}$ & $C_{d_{friction}}$ ***Fig****.[4a, 4b]*. The average pressure drag component contribution is found to be 75.48 % and friction drag to be 24.52 %. The $C_{d_{Pressure}}$ (85 %) and $C_{d_{Friction}}$ (15%) is confirmed in [2] with $R_{e_{\sqrt{L}}}$ (L = Ahmed body length) which is lower compared to present study, implying $C_{d_{Pressure}}$ contribution reduces with increase in R_e. The lowest $C_{d_{Total}}$ is observed at 9° i.e., 105.5 drag counts lesser compared to 35°, closer to 10° observed in [3] for same $R_{e_{\sqrt{A}}}$. At 9° the $C_{d_{pressure}}$ (73.965 %) is lowest but the $C_{d_{friction}}$ (26.03 %) is among the highest. At ϕ = 9° the flow is completely attached on the slant surface accounting for highest skin friction contribution whereas the two wake re-circulations only affected the flow on the back surface and are confined by the bottom and the top downstream flow. Hence, resulting in lowest form/pressure drag and friction drag combination. Contrary to 9°, the highest $C_{d_{Total}}$ is observed at 53° i.e 21.9 drag counts with highest contribution of $C_{d_{Pressure}}$ (77 %) and lowest $C_{d_{friction}}$ (23 %).

Above the critical angle (ϕ_{cr}) = 30° till (ϕ) = 41° the $C_{d_{Total}}$ increase is gradual and below 7 drag counts. The consistency in $C_{d_{Total}}$ value for slant angle $30° < (\phi) < 41°$ is due to the successive reduction in the back-surface height for this range of ϕ, moving the upper re-circulation completely above

the slant surface leading flow separation from slant leading edge [2], ***Fig. 5***.

Below (ϕ_{cr}) the steep fall is observed in the till (ϕ) = 12.5°, ***Fig***. *[3a, 4a]*, hence confirming the two critical angles for flow behavior changes (ϕ_{cr}) = 12.5° and (ϕ_{cr}) = 30°. The flow over most of the slant (except side edge) for $\phi \leq 12.5°$ fairly seems 2D [2]. The wake structure consisted of two contra rotating re-circulating vortex, upper and lower, ***Fig***. *5* with completely attached flow over slant surface for 9° <= ϕ <= 12.5°, whereas above 12.5° and especially at 17° flow reversal is observed over the slant surface leading to sudden drag rise above $\phi \geq 12.5°$. The re-circulation bubble begins to form at 17° at slant surface trailing edge and continue to grow $\phi \leq 41°$ which aided in energizing the upper re-circulation zone resulting in lesser ($C_{d_{friction}}$) and remarkable rise in $C_{d_{pressure}}$, ***Fig***. *5*. Increase in $\phi \geq 17°$ showed direct correlation with the strength of longitudinal slant side vortices which amplified the upper re-circulation giving a 3D structure (horseshoe vortex) to the entire wake. This horseshoe vortex has the most pronounced effect in the wake structure, increment of $C_{d_{pressure}}$ and decrement of $C_{d_{friction}}$ effects of which can be seen on C_p in *Fig. [1c, 1d, 2b]* . The phenomena of merging of separation region on slant reduces the influence of side edge vortices [2] leading to less obstruction to upcoming flow.

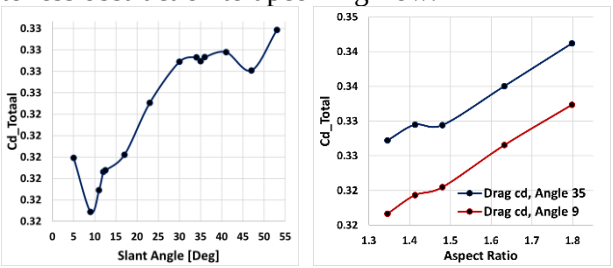

Fig. **3:** $C_{d_{total}}$ and Aspect Ratio (AR*) influence 35° & 9°

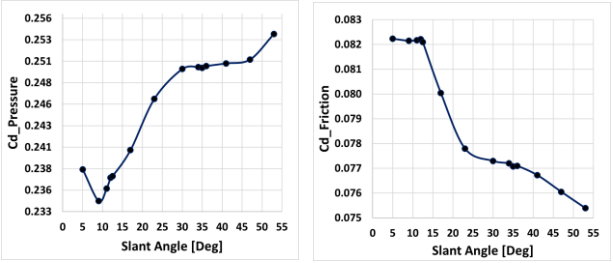

Fig. **4:** Pressure and Friction drag variations with ϕ

The investigation of AR* highlighted linear progression of $C_{d_{total}}$, ***Fig***. 3b. The increment in surface area of the Ahmed body showed good correlation with the size of the wake structure. The proportionate increment in surface area and wake size results in increase of the $C_{d_{pressure}}$ and decrease in $C_{d_{friction}}$ linearly. The trend is a consistent off-set of [3.22 to 2.59] drag counts from lowest to highest aspect ratio for 9° w.r.t 35°, but importantly followed the same behavior as 35°. The results in *Fig. 3b* agree well with observations made in [3], where narrower body showed increased circulation which promotes flow reattachment over slant hence reducing $C_{d_{total}}$.

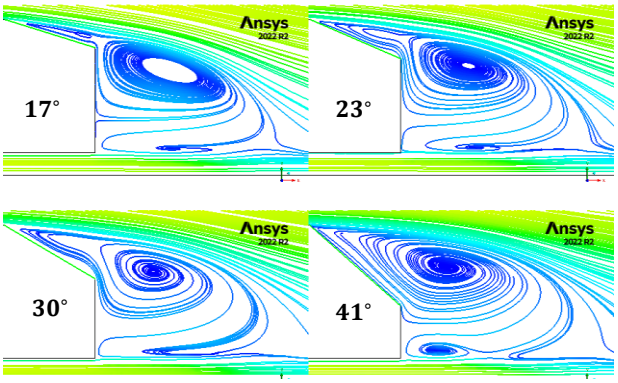

Fig. **5:** Velocity streamlines displaying wake re-circulation

CONCLUSONS

The present study aimed to estimate minimum (best) and maximum (worst) drag coefficient ($C_{d_{Total}}$) value for a range of slant angle of the Ahmed body. (1) The validation for $C_{d_{Total}}$ and $C_{l_{Total}}$ for each surface against LES data showed good agreement for $C_{d_{Total}}$ ϕ = 35°. (2) The best slant angle is $\phi = 9°$ and worst is $\phi = 53°$ (highest ϕ in this study). (3) The critical angles where flow behavior change is observed to be at $\phi = 12.5°$ & $\phi = 30°$. (4) Constant $C_{d_{Total}}$ observed for $30° \leq \phi \leq 41°$ range. (5) The re-circulation bubble is detected for $17° \leq \phi < 41°$ on slant surface. (6) Aspect ratio increase ($1.3 \leq AR \leq 1.8$) promotes flow separation hence $C_{d_{Total}}$ rise.

REFERENCES

[1] Tural Tunay, Besir Sahin, Veli Ozbolat. Effects of rear slant angles on the flow characteristics of Ahmed body, Elsevier, 2014.

[2] Ahmed, S. R., Ramm, G., & Faltin, G. (1984). Some Salient Features of the Time -Averaged Ground Vehicle Wake. *SAE Transactions*, *93*, 473–503. http://www.jstor.org/stable/44434262

[3] James Venning, David Lo Jacono, David Burton, Mark C. Thompson, John Sheridan. The effect of aspect ratio on the wake of the Ahmed body. Experiments in Fluids, 2015, vol. 56 (n° 6), pp. 1-11. ff10.1007/s00348-015-1996-5ff. ffhal-01167075